Published in final edited form as:
Thromb Haemost. 2009 December ; 102(6): 1169–1175. doi:10.1160/TH09-03-0199.

Fibrin network structure and clot mechanical properties are altered by incorporation of erythrocytes

Kathryn C. Gersh, **Chandrasekaran Nagaswami**, and **John W. Weisel**
Department of Cell and Developmental Biology, University of Pennsylvania School of Medicine, Philadelphia, Pennsylvania, USA

Summary

Although many *in vitro* fibrin studies are performed with plasma, *in vivo* clots and thrombi contain erythrocytes, or red blood cells (RBCs). To determine the effects of RBCs on fibrin clot structure and mechanical properties, we compared plasma clots without RBCs to those prepared with low (2 vol%), intermediate (5–10 vol%), or high (≥20 vol%) numbers of RBCs. By confocal microscopy, we found that low RBC concentrations had little effect on clot structure. Intermediate RBC concentrations caused heterogeneity in the fiber network with pockets of densely packed fibers alongside regions with few fibers. With high levels of RBCs, fibers arranged more uniformly but loosely around the cells. Scanning electron micrographs demonstrated an uneven distribution of RBCs throughout the clot and a significant increase in fiber diameter upon RBC incorporation. While permeability was not affected by RBC addition, at 20% or higher RBCs, the ratio of viscous modulus (G″) to elastic modulus (G′) increased significantly over that of a clot without any RBCs. RBCs triggered variability in the fibrin network structure, individual fiber characteristics, and overall clot viscoelasticity compared to the absence of cells. These results are important for understanding *in vivo* clots and thrombi.

Keywords

Blood coagulation; confocal microscopy; erythrocyte; fibrin; fibrin network

Introduction

Erythrocytes, or red blood cells (RBCs), play a role in blood coagulation by increasing blood viscosity, which is associated with a propensity for clot formation (1–3). In diseases such as polycythemia, this increase in viscosity leads to a greater risk of thrombosis (4). Another prothrombotic role of RBCs is their haemodynamic tendency to move toward the center of a vessel during flow, pushing the smaller, lighter particles such as platelets toward the periphery, where they are more easily activated upon vessel injury (5,6). Thus, anaemic patients with severely diminished haematocrit levels often display delayed clotting times and a bleeding tendency (7), and stored RBCs that have lost their deformability do not facilitate coagulation upon transfusion as well as do freshly prepared RBCs (8). RBCs can express phosphatidylserine on their surface, providing an active surface to trigger coagulation in some disease states that predispose patients for thrombosis, such as sickle cell anaemia (9). Alterations in RBC structure, as also occur with disseminated intravascular coagulation and haemolytic anaemia, may also lead to thrombosis (10,11).

Correspondence to: John W. Weisel, Department of Cell and Developmental Biology, University of Pennsylvania School of Medicine, 1054 BRB II/III, 421 Curie Blvd, Philadelphia, PA 19104–6058, USA, Tel.: +1 215 898 3573, Fax: +1 215 898 9871, weisel@mail.med.upenn.edu.

Despite their significance in thrombosis and haemostasis, relatively few studies have been conducted to describe the effects of RBCs on fibrin clot structure. One complication of studying RBC-rich thrombi is that incorporation of RBCs into a thrombus is uncontrolled and variable. For example, a recent investigation of thromboemboli removed from acute ischaemic stroke patients revealed that while all of the same components (fibrin, blood cells, etc) could be found in each thrombus, each one displayed remarkable variation in overall appearance (12). Another reason for this scarcity may be, in part, due to the fact that the presence of RBCs in a clot often interferes with the laboratory technique being used to probe clot structure, such as turbidity.

To circumvent this problem, Carr and Hardin used perfusion to probe the structure of whole blood clots (13). Because RBCs percolated through the clot during permeation, the diameter of the RBC could be used as a probe for pore size, even though the cells deformed while passing through the clot. They concluded that the presence of RBCs does not change fibrin mass to length ratio, but does increase pore size in a non-concentration-dependent manner (13). Van Gelder et al. later performed similar permeability experiments, but unlike Carr and Hardin, did not experience RBC washout (14). When RBCs were added, they found a decrease in the permeability of fibrin clots that was proportional to both the total RBC surface area and their total concentration. Based on these results, they suggested that RBCs form clumps and rouleaux when incorporated into a clot network (14).

While these two studies employed elegant methods to derive information about clot structure, the approaches were indirect. With current microscopes and labelling strategies, we can now directly observe the effects of RBC incorporation on fibrin clot structure. We have visualised RBC-containing clots by scanning electron microscopy and fluorescent confocal microscopy. In addition to this direct investigation of the effect of RBCs on clot structure, we have also probed the ways in which RBC addition can change the biophysical properties of the clot, such as permeability and viscoelasticity. We demonstrated that addition of RBCs leads to heterogeneity in fibrin network structure and modulation of network stiffness, but that the specific effects of RBCs depend in a complex way upon the concentration of cells.

Materials and methods

Preparation of human platelet-poor plasma and RBCs

Human platelet-poor plasma (PPP) was prepared by collecting whole blood into sodium citrate (10 mM final concentration). Immediately after collection, samples were spun at room temperature for 15 minutes at 130–160 g, and then the supernatant was spun down at 10,000 g for 10 min and pooled. Whole blood for RBC preparation was obtained by finger puncture and drawn directly into RBC wash buffer [3% bovine serum albumin (BSA), 5 mM glucose, 9 mM $CaCl_2$, 5 mM $MgCl_2$ in Dulbecco's phosphate buffered sodium (PBS) (Invitrogen, Carlsbad CA, USA)]. The blood was immediately spun down at room temperature at 1,200g for 4 min, then the RBC pellet was washed four times with 15 volumes of RBC wash buffer by resuspension and centrifugation. At this point, RBCs could be stored in RBC wash buffer for up to 24 hours (h) with no visible haemolysis. The stock suspension remaining after removal of the last batch of wash buffer was 100% RBCs (% RBCs in all solutions were measured by volume). When necessary, RBC preparations were labelled according to the manufacturer's protocol with Vybrant DiD cell-labelling solution (Molecular Probes, Eugene, OR, USA) that had a maximum absorbance at 647 nm. The same viscoelastic properties were demonstrated by rheometry (as described below) for clots prepared with RBCs derived using this finger stick protocol as for those containing the same amount of RBCs derived from venipuncture.

Confocal microscopy

Fibrin clots were prepared in a total volume of 100 μl using PPP mixed with 0.075 μM (final conc.) Alexa 488-labelled human fibrinogen (purchased from Molecular Probes, with molar ratio of dye to protein of 8:1). PPP (80 μl) was mixed with appropriate volumes of 100% DiD-labelled RBCs and/or buffer (20 mM HEPES pH 7.4, 150 mM NaCl [HBS]) for final concentrations of 0, 2, 10, and 20% RBCs. Samples contained 5% Gloxy anti-fade reagent (8% glucose, 3.3 U/μl glucose oxidase, 52 U/μl catalase in HBS) to reduce photobleaching. Clot formation was initiated by addition of thrombin and $CaCl_2$ to final concentrations of 0.5 U/ml and 20 mM, respectively. Thin (~200 μm) chambers were prepared by affixing three layers of double-sided tape to a microscope slide to form three sides of a ~1 × 2 cm rectangle. A #1.5 coverslip was placed over the tape to form the chamber that was then filled with sample and sealed with grease. Chambers were incubated on a rotator at 8 rpm at room temperature for 1 h during clot formation to keep RBCs from settling. Confocal images were obtained on a Zeiss Axiovert inverted confocal microscope with a 63X, 1.2 NA water lens using a 488 nm Argon laser or a 633 nm HeNe laser (Carl Zeiss Micro-Imaging Inc, Thornwood, NY, USA). A 10 μm stack was obtained with 0.5 μm slices starting at 30 μm above the coverslip (10 μm above for the 20% sample because of darkening due to the RBCs). Gain and offset were adjusted for each image so that 1% of total pixels were saturated and 1% of pixels were zero.

Scanning electron microscopy

Clots were prepared in PPP with the appropriate amount of RBCs for final concentrations of 0, 2, 10, and 20% RBCs. Clot formation was initiated by the addition of thrombin and $CaCl_2$ to final concentrations of 0.5 U/ml and 20 mM, respectively. Two microchambers were filled with each sample, and these chambers were loaded into a 15 ml conical tube packed with moist Kimwipes and rotated at 8 rpm at room temperature for 1 h to prevent RBC settling. Chambers were transferred into a 50 ml conical tube attached to the rotator; the tube was filled three times with HBS and three times with cacodylate buffer (15) over several hours to wash the clots, and then they were fixed in 2% glutaraldehyde. Fixation, dehydration, sample preparation, and microscopy on a Phillips/FEI XL20 scanning electron microscope (FEI Company, Hillsboro, OR, USA) were performed according to the method of Weisel and Nagaswami (15).

Image analysis

Image files were opened and manipulated in Image J (Wayne Rasband, NIH). In each confocal microscopy experiment (n=3), one image that looked least like its neighbours was chosen to discard as an outlier before analysis. Measurements were performed on a 126X magnification image. Slices were flattened into a sum z-projection, and divided into a 64-square grid to measure the number of fibers visible in each square and the density of protein in a square based on image brightness. Fiber diameters were measured on high definition scanning electron micrographs of 1,000X magnification (digitally zoomed to 6,000X) by drawing a line to bisect a foreground fiber and measuring its length in Image J.

Clot permeability

Fibrin clot permeability was measured with a few differences from the method of Marchi et al. (16). In brief, clots were prepared from 70 μl PPP, 1 U/ml thrombin, 20 mM $CaCl_2$, and RBCs or HBS to bring sample volume to 100 μl and % RBCs to 0, 2, 5, 10, 15, or 20%. These clots were formed in small chambers prepared from 3 mm inner diameter plastic tubes, and were incubated for 1 h at room temperature on a rotator at 8 rpm to prevent RBC settling prior to being set up on the flow apparatus. Once the clot had formed, 11 ml buffer was allowed to flow through to wash out any loose RBCs. When a constant flow of buffer was established, flow-through was collected for 30 min. The volume of buffer that passed through the column

in this amount of time was used to calculate permeability constant according to the Darcy equation:

$$K_s=[Q*L*n]/[t*A*\Delta P]$$

where Q = flow-through volume (ml); L = clot length (cm); n = buffer viscosity [g/(cm*s)]; t = time of volume collection (sec); A = clot cross-sectional area (cm^2); ΔP = differential pressure ($dynes/cm^2$).

Viscoelastic measurements

Clots for viscoelastic measurements were prepared from 40 μl PPP, 1 U/ml thrombin, 20 mM $CaCl_2$, and appropriate volumes of RBCs and HBS to bring the final sample volume to 100 μl with 0, 5, 10, 20, 30, 40, or 50% RBCs. Samples were prepared between glass slides attached to the 8 mm diameter parallel plate of an RFS II Rheometer (TA Instruments, New Castle, DE, USA). The plates were adjusted so that the exposed sides of the clot were perpendicular to the plates, not concave or convex. After 1 h of incubation, a strain-controlled dynamic time sweep test was performed with a frequency of 5 radians/second, 2% strain, and readings every 15 seconds for 1 min. The first reading was discarded and the remaining four averaged to determine G′ (elastic modulus), G″ (viscous modulus), and tan δ [ratio of viscosity (G″) to elasticity (G′)], as calculated by the TA Orchestrator software.

Results

Confocal microscopy of PPP clots with varying percentages of RBCs

With fluorescent confocal microscopy, we directly addressed the role of RBCs on fibrin clot structure. By labelling the fibers in a clot with fluorescent fibrin(ogen) and imaging with a laser scanning confocal microscope, we could allow RBCs to remain in our samples, but visualise just the naturally hydrated fiber network, without having our view obstructed by RBCs. To locate the RBCs themselves, we imaged them in a separate wavelength channel and overlaid the images after acquisition. We took 10 μm stacks with 0.5 μm slices, and sum Z-projections of these stacks are shown in Figure 1. While adding RBCs did not appear to change the small-scale structural features of the fibers, the overall appearance of the clot did change as more RBCs were incorporated. Upon addition of 10% RBCs, the clot structure became more non-uniform with densely packed fiber regions as well as large holes where more RBCs were situated. When 20% RBCs were included, fibers were much less densely packed than in clots lacking RBCs. Because the masses of cells blocked light to the sample, we could not visualise samples that contained more than 20% RBCs.

We performed a quantitative analysis of the fibrin network structure for each set of confocal images, and results of one representative analysis are shown in Table 1A. Onto the sum Z-projection of the fiber channel only, we placed a 64-box grid in Image J, and in each square counted the number of fibers and measured protein density as indicated by brightness. The main characteristic we observed by eye was a striking heterogeneity between dense network and holes. Simply averaging fiber number and protein density obscured these differences, so we divided the 64 boxes evaluated in each image into quartiles. Next we calculated the difference between the average of the highest quartile of values and the average of the lowest quartile. A large number for this calculation would indicate that the clot being analysed is heterogeneous, while a lower value would describe a clot with a more homogeneous distribution of fibers.

Because we varied the confocal microscope gain and offset settings from day to day in order to best image the prepared samples, these calculated difference values could not be directly

averaged for the three separate experiments. Thus we determined the % change in difference values for each condition compared to its own control. From these % change values, we could calculate averages and standard errors of the effect of RBCs on fibrin clot heterogeneity (Table 1B). Although none of the values were statistically significant, we found that addition of 2% RBCs had no effect on the fiber number difference, but addition of 10 or 20% RBCs did increase this parameter. When we measured protein density by brightness of the square, rather than by fiber number, we found the same pattern of a large spike in density difference value for 10% RBCs, a smaller increase for 20% RBCs, and no change for 2% RBCs.

Scanning electron microscopy of PPP clots with varying percentages of RBCs

We used scanning electron microscopy to obtain higher resolution data about the fibrin network and fiber structure upon addition of RBCs. Upon direct visual examination of the clots prepared for this technique, we noted the RBCs tended to be heterogeneously arrayed throughout the sample. Figure 2 (0%) shows a representative micrograph of a dense clot formed without RBCs from PPP, visualised at 1,000X magnification. Addition of 2% RBCs to the fibrin clot caused fiber thickening, but minimal disruption in the clot network with RBCs inserting into pores (Fig. 2, 2%). Addition of 10% or 20% RBCs led to much more extensive network rearrangement. In both sets of images we observed clumps of RBCs interspersed between bundles of fibers (Fig. 2, 10%, 20%). Packing of fibers appeared much less dense with larger pores in the presence of RBCs than in their absence.

We observed that addition of any amount of RBCs clearly increased average fibrin fiber diameter. We also found a significant difference in control fiber diameters between preparation dates that was likely due to the use of different thrombin stocks or other variables. This very common experience over years of work with scanning electron micrographs of fibrin clots has taught us that it is better to focus on differences between experimental and control samples from each preparation than on the absolute differences between samples prepared at different times. Therefore, to remove the effect of variability in sample preparation, we compared the fiber diameters measured for each sample with the average fiber diameter calculated for that day's control sample, yielding the % difference from control fiber diameter for each sample. Table 2 shows the average ± standard error for the % difference from control for each % RBCs (4 clots with 2–5 images acquired per clot, and ~500 total fibers measured). Addition of 2% RBCs yielded 11% ± 4% thicker fibers ($p < 0.01$); with 10% RBCs, fiber thickness increased by 17% ± 6% ($p < 0.01$); and 20% RBCs yielded 20% ± 12% thicker fibers ($p < 0.05$).

Clot permeability

To determine the effect of RBCs on fibrin clot mechanical properties, we measured clot permeability in a manner similar to that used by Carr and Hardin (13). After clot formation on the rotator to prevent settling of the RBCs, we washed with HBS and as previously shown (13), found that buffer flow rate increased to a plateau as RBCs were washed from the clot. Almost 100% of added RBCs were recovered in the eluate. The increase in flow rate did not take place while washing the 0% RBC clot (data not shown). Once a standard amount of HBS had passed through each clot and RBCs were flushed out, we measured permeability through the resulting fiber network for 30 min. As shown in Figure 3, there were no significant differences in permeability constant (K_s) for any of the samples tested ($p > 0.15$ using independent t-test). We tried to measure permeability of clots containing 50% RBCs, but they did not attach tightly enough to the walls of the permeation chamber and were flushed out during the initial wash.

Viscoelastic measurements

Unlike the clots prepared for imaging that were formed on a rotator to keep RBCs evenly distributed throughout the network, clots prepared for viscoelastic measurements need to be

formed between the fixed plates of the rheometer. Since the clots could not be rotated, we doubled the concentration of thrombin (from 0.5 U/ml to 1 U/ml) to approximately double the rate of clot formation and quickly "trap" RBCs in the network to keep them from settling to the bottom. Using this method, no variations in RBC concentration over the height of the clot were visible by eye. Control confocal microscopy experiments indicated that the effect of RBCs on clot structure was the same for clots formed from 1 U/ml thrombin as for those formed from 0.5 U/ml thrombin. We found that the clots containing RBCs exhibited biphasic behavior with respect to both elastic and viscous properties as a function of RBC concentration (Fig. 4A). The elastic modulus increased up to addition of 10% RBCs, but then decreased again below its baseline with addition of higher percentages of RBCs. The viscous modulus similarly increased to a peak at 10% RBCs, and then decreased, but never below its initial 0% value. The ratio of viscous to elastic component, tan δ, increased upon addition of 10% or more RBCs (Fig. 4B). Compared to the tan δ of a clot without RBCs, the values for 20% – 50% RBCs were significantly higher ($p < 0.05$ using independent t-test).

Discussion

We investigated the structure and properties of plasma clots formed *in vitro* in the presence of RBCs to determine the effect these cells might have on fibrin structure *in vivo*. It is important to note that these results are biologically and clinically relevant since clots and thrombi can have widely different concentrations of RBCs incorporated. We found that the presence of RBCs increased clot heterogeneity, both by their degree of incorporation and in the network structure itself. From images obtained by both scanning electron and confocal microscopy of clots formed in the presence of variable concentrations of RBCs, it is clear that RBCs are incorporated into the spaces between fibers where they can cause some amount of disruption in the gross fibrin network structure. Regions of greater and lesser RBC density are even visible to the naked eye during scanning electron microscopy sample preparation. Addition of 10% RBCs to the clots monitored by confocal microscopy increased network heterogeneity, an effect that was notable by eye and quantifiable (though not statistically significant) by measuring fiber number differences and protein density differences over small regions throughout the clot. Below this concentration, RBCs fit into existing holes in the network without disrupting it. Above it, RBCs fully incorporate into the clot, decreasing fiber density throughout the entire network. Although the two microscopy techniques do not yield identical results because of differences in sample hydration and location of monitoring (surface for scanning electron microscopy and internal for confocal microscopy), the results of both methods reveal heterogeneity of RBC incorporation into the clots, emphasising the advantages of combining different types of microscopy to utilise the strengths of each.

In addition to fiber arrangement, RBCs also affected fiber formation, as demonstrated by the increased fiber diameters measured in scanning electron micrographs upon addition of any amount of RBCs. Because thicker fibrin fibers are often found at the expense of highly branched networks (17), we propose that RBCs block branch protrusion when they surround growing fibers. Instead, monomers tend to align with pre-existing fibers leading to thick fibers in an open, porous network. We have shown that addition of RBCs to a fibrin clot affects clot structure by disrupting fibrin structure through crowding as if the cell were an inert disk, while influencing clot mechanical properties through the viscoelastic properties of the cells themselves.

RBCs exert this influence on clot mechanical properties through their high deformability (18,19). While microscopy is best suited for characterisation of the details of fibrin clot structure, measurement of mechanical properties reflects the behavior of the clot as a whole. In the experiments described, elastic and viscous moduli moved in parallel, increasing to peaks at 10% RBCs, and then both decreasing as more RBCs were included in the clot. This biphasic

behavior likely arises from the contribution of the changing fibrin network at low RBC concentrations, and then as the RBC concentration increases, their own very complex viscoelastic properties predominate (20–22). The viscous nature of a sample packed with RBCs and their increasing contribution to the clot's overall viscoelasticity leads to a tendency toward irreversible deformation. This behavior is also reflected in the ratio of viscous to elastic moduli, tan δ, which increased with addition of RBCs, significantly for 20% or more cells. Packing more RBCs into the network eventually becomes overwhelming and disrupts the integrity of the network as seen on the confocal microscope with the loosely packed 20% RBC clots. At this point, RBCs take over as the major component of the clot. Although we cannot visualise them, we predict that clots formed with 50% RBCs would have even looser fiber packing. The clumps of RBCs are so large that an extensive, uniform fibrin network cannot form, resulting in a highly viscous clot.

Our results suggest that permeability is not, in fact, a good determinant of clot structural changes upon incorporation of RBCs. Even though we observed clear structural effects by confocal and electron microscopy and measured changes in viscoelastic behavior, permeability of a clot did not change when different amounts of RBCs were incorporated. Importantly, permeability experiments were performed after RBCs were washed from the prepared clot, while they remained present during each of the other techniques. Perhaps the local differences observed in structure are cancelled out over the entirety of the clot. Our results differ somewhat from those of Carr and Hardin who found an increase in permeability rate and thus pore size, but no change in fiber mass to length ratio when RBCs were present (13). We propose that this discrepancy is due to different experimental conditions between our protocol and that used by Carr and Hardin. They used water to haemolyse RBCs during the later stages of flow measurements, while we continued permeation with buffer to prevent haemolysis. In addition, they did not rotate the sample during its 1-h incubation which would have allowed a significant portion of the RBCs to settle near the bottom of the clot, significantly disrupting fibrin network structure in this region.

In summary, the incorporation of RBCs into a fibrin clot significantly affects clot structure and mechanical properties in a concentration-dependent manner. Thus the effect of RBCs on fibrin structure is an important factor to consider when extrapolating findings from studies of plasma clots to *in vivo* systems. Another such factor is the effect of flow on clot structure, but that was beyond the scope of this study. Although the magnitudes of some of the measured changes are rather small, differences of similar size can be observed when measuring mechanical and morphological properties of the plasma of healthy subjects compared to coronary artery disease patients, suggesting that even small structural differences can have a large influence on pathophysiology (23,24). The effects of RBCs are largely based on the heterogeneity of incorporation, which is not an experimental artifact, but representative of the varying structures of thrombi found in arteries versus veins, or in the occlusive thrombi removed from patients (12). From our evidence on a purified system, we hypothesise that the degree and pattern of incorporation of RBCs into pathologic thrombi will influence the viscoelastic properties and resulting pathological consequences associated with these thrombi.

What is known about this topic?

– Red blood cells (RBCs) play a prothrombotic role in blood coagulation by increasing blood viscosity and forcing platelets toward the vessel well.

– By measuring buffer percolation through clots formed from whole blood, RBCs were shown to increase pore size in a fibrin network.

– Later permeability experiments suggested that RBCs collect into clumps and rouleaux inside a fibrin network.

What does this paper add

– Direct visualisation by confocal and scanning electron microscopy demonstrates that low concentrations of RBCs incorporate heterogeneously into a fibrin network, while higher concentrations are more uniformly arranged.

– Addition of any amount of RBCs leads to formation of thicker fibrin fibers and influences clot viscoelasticity by increasing the viscous component of the sample relative to the elastic.

Acknowledgments

This study was funded by NIH grants: NIH T32 H107971 (KCG) and NIH HL30954 (JWW).

The authors thank May Thu Saung for expert technical assistance and Dr. Rustem Litvinov for critically reading the manuscript. This work was supported by NIH grants HL30954 and T32 H107971.

References

1. Wohner N. Role of cellular elements in thrombus formation and dissolution. Cardiovasc Hematol Agents Med Chem 2008;6:224–228. [PubMed: 18673236]
2. Zannad F, Stoltz JF. Blood rheology in arterial hypertension. J Hypertens Suppl 1992;10:S69–78. [PubMed: 1403236]
3. Schmid-Schonbein H, Wells R, Goldstone J. Influence of deformability of human red cells upon blood viscosity. Circ Res 1969;25:131–143. [PubMed: 5806159]
4. Landolfi R, Rocca B, Patrono C. Bleeding and thrombosis in myeloproliferative disorders: mechanisms and treatment. Crit Rev Oncol Hematol 1995;20:203–222. [PubMed: 8748010]
5. Goldsmith HL. Red cell motions and wall interactions in tube flow. Fed Proc 1971;30:1578–1590. [PubMed: 5119364]
6. Goldsmith HL, Bell DN, Braovac S, et al. Physical and chemical effects of red cells in the shear-induced aggregation of human platelets. Biophys J 1995;69:1584–1595. [PubMed: 8534829]
7. Hellem AJ, Borchgrevink CF, Ames SB. The role of red cells in haemostasis: the relation between haematocrit, bleeding time and platelet adhesiveness. Br J Haematol 1961;7:42–50. [PubMed: 13713094]
8. Reinhart WH, Zehnder L, Schulzki T. Stored erythrocytes have less capacity than normal erythrocytes to support primary haemostasis. Thromb Haemost 2009;101:720–723. [PubMed: 19350117]
9. Zwaal RF, Schroit AJ. Pathophysiologic implications of membrane phospholipid asymmetry in blood cells. Blood 1997;89:1121–1132. [PubMed: 9028933]
10. Ataga KI, Orringer EP. Hypercoagulability in sickle cell disease: a curious paradox. Am J Med 2003;115:721–728. [PubMed: 14693325]
11. Levi M, Ten Cate H. Disseminated intravascular coagulation. N Engl J Med 1999;341:586–592. [PubMed: 10451465]
12. Marder VJ, Chute DJ, Starkman S, et al. Analysis of thrombi retrieved from cerebral arteries of patients with acute ischemic stroke. Stroke 2006;37:2086–2093. [PubMed: 16794209]
13. Carr ME Jr, Hardin CL. Fibrin has larger pores when formed in the presence of erythrocytes. Am J Physiol 1987;253:H1069–1073. [PubMed: 3688251]
14. van Gelder JM, Nair CH, Dhall DP. The significance of red cell surface area to the permeability of fibrin network. Biorheology 1994;31:259–275. [PubMed: 8729486]
15. Weisel JW, Nagaswami C. Computer modeling of fibrin polymerization kinetics correlated with electron microscope and turbidity observations: clot structure and assembly are kinetically controlled. Biophys J 1992;63:111–128. [PubMed: 1420861]
16. Marchi R, Lopez Ramirez Y, Nagaswami C, et al. Haemostatic changes related to fibrin formation and fibrinolysis during the first trimester in normal pregnancy and in recurrent miscarriage. Thromb Haemost 2007;97:552–557. [PubMed: 17393017]

17. Ryan EA, Mockros LF, Weisel JW, et al. Structural origins of fibrin clot rheology. Biophys J 1999;77:2813–2826. [PubMed: 10545379]

18. Banerjee R, Nageshwari K, Puniyani RR. The diagnostic relevance of red cell rigidity. Clin Hemorheol Microcirc 1998;19:21–24. [PubMed: 9806729]

19. Dobbe JG, Hardeman MR, Streekstra GJ, et al. Analyzing red blood cell-deformability distributions. Blood Cells Mol Dis 2002;28:373–384. [PubMed: 12367581]

20. Evans EA, La Celle PL. Intrinsic material properties of the erythrocyte membrane indicated by mechanical analysis of deformation. Blood 1975;45:29–43. [PubMed: 803108]

21. Yoon YZ, Kotar J, Yoon G, et al. The nonlinear mechanical response of the red blood cell. Phys Biol 2008;5:36007.

22. Mohandas N, Gallagher PG. Red cell membrane: past, present, and future. Blood 2008;112:3939–3948. [PubMed: 18988878]

23. Collet JP, Allali Y, Lesty C, et al. Altered fibrin architecture is associated with hypofibrinolysis and premature coronary atherothrombosis. Arterioscler Thromb Vasc Biol 2006;26:2567–2573. [PubMed: 16917107]

24. Sjoland JA, Sidelmann JJ, Brabrand M, et al. Fibrin clot structure in patients with end-stage renal disease. Thromb Haemost 2007;98:339–345. [PubMed: 17721616]

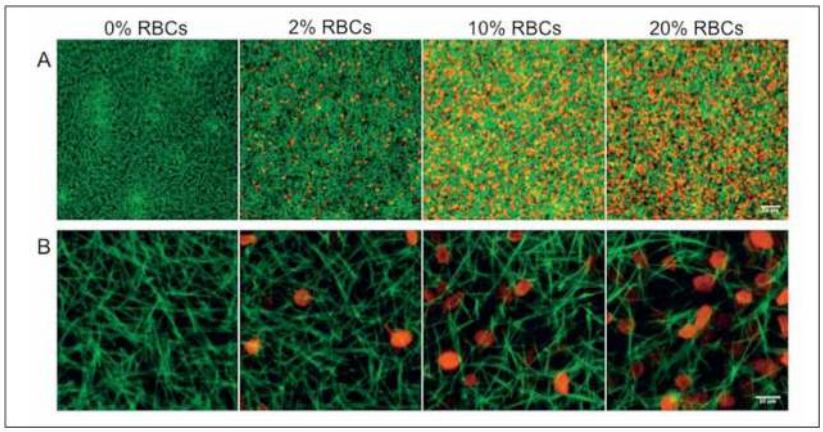

Figure 1. Confocal images of RBC-containing clots

Clots formed with 0.5 U/ml thrombin, 20 mM $CaCl_2$, and 0, 2, 10, or 20% RBCs (by volume) with two labels. Alexa 488-labelled fibrin fibers are shown in green, while Vybrant DiD-labelled RBC membranes are shown in red. A) 20X, magnification bar = 50 μm; B) 126X, magnification bar = 10 μm.

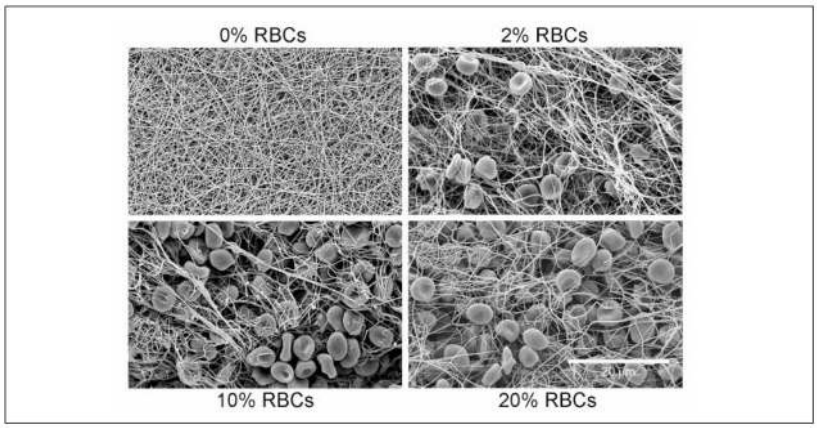

Figure 2. Scanning electron micrographs of RBC-containing clots

Clots formed with 0%, 2%, 10%, and 20% RBCs (by volume) with 20 mM $CaCl_2$ and 0.5 U/ml thrombin. Clots were prepared in chambers that were rotated during clot formation, washing, and fixing to prevent RBC settling. Images shown in this figure were taken at 1,000X; magnification bar = 20 μm.

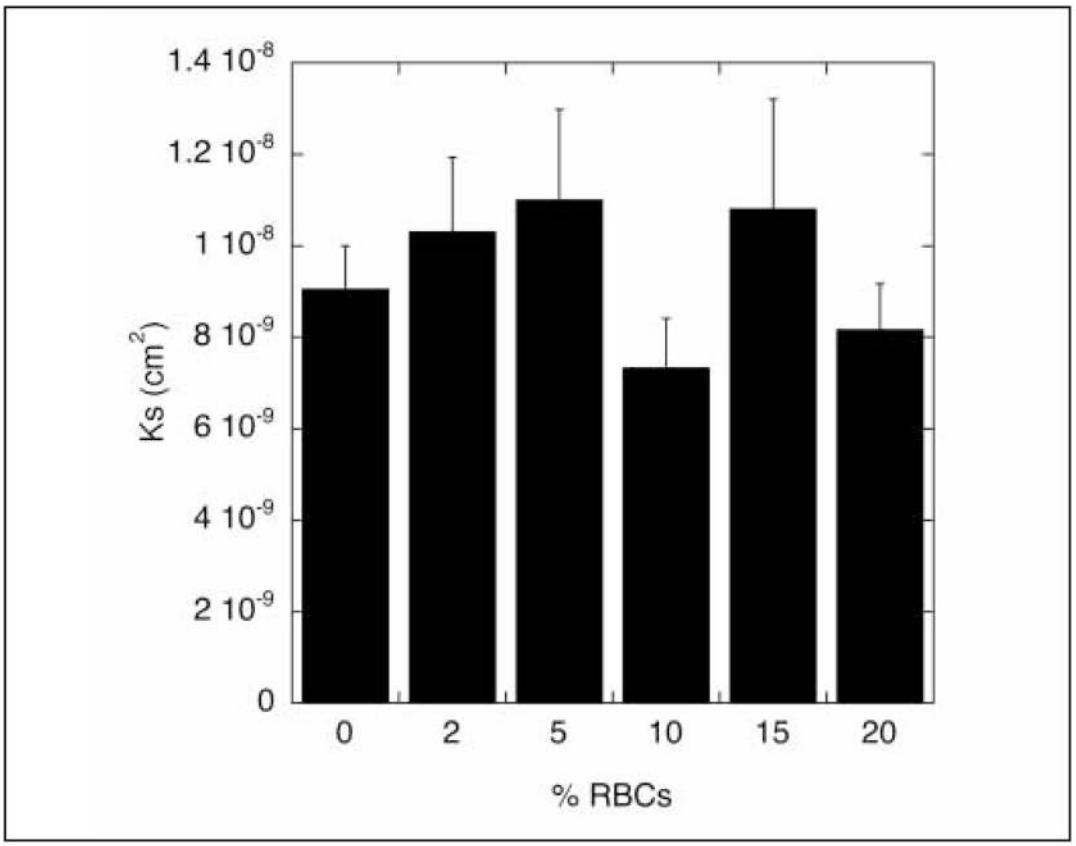

Figure 3. Permeability of RBC-containing clots

Clot permeability was measured by flow of HBS through a clot for 30 min. Free RBCs were washed out with HBS prior to measurement. The permeability constant was calculated according to the Darcy equation (see *Methods*). Data are plotted as mean ± standard error of the mean (n=5–8), and $p > 0.15$ for all comparisons (independent t-test).

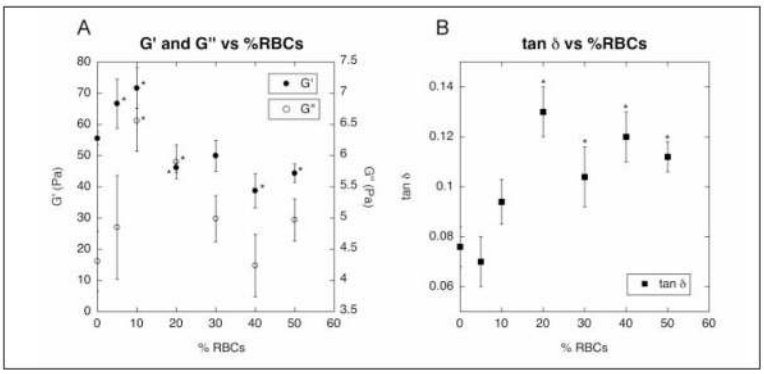

Figure 4. Viscoelastic measurements of RBC-containing clots

Viscoelastic measurements were performed on clots formed from PPP with 0 – 50% RBCs (by volume) with 20 mM $CaCl_2$ and 1 U/ml thrombin on a TA Instruments RFS II Rheometer. G ′ and G″ values are shown in plot A, and tan δ values are shown in plot B. Data are plotted as mean ± standard error of the mean (n=5–10). * $p < 0.05$ for comparison with 0% RBCs (using independent t-test).

Table 1

Analysis of confocal images of RBC-containing clots

A) The average fiber number and brightness for the densest and sparsest quartiles of 64 measured grid squares overlaying an image are shown. The difference between these two values reflects the relative heterogeneity of the sample. Means are listed ± standard deviation for six images of each sample. The data shown in part A come from one analysis, representative of three individual experiments. B) We determined for each experiment the % change in heterogeneity values for the presence of RBCs compared to the 0% RBC control; they are shown as average ± standard error of the mean (n=3). P-values were determined by independent Student's t-test.

A)						
% RBCs	Fiber number			Protein density		
	Dense quartile	Sparse quartile	Difference	Dense quartile	Sparse quartile	Difference
0%	8.7 ± 1.4	3.4 ± 0.9	5.3 ± 0.4	733 ± 117	316 ± 60	418 ± 47
2%	8.3 ± 1.3	3.2 ± 1.0	5.1 ± 0.5	742 ± 112	321 ± 69	422 ± 36
10%	9.3 ± 1.6	2.6 ± 1.5	6.7 ± 0.6	922 ± 233	295 ± 146	627 ± 70
20%	10.5 ± 1.9	3.6 ± 1.1	6.9 ± 1.6	781 ± 128	310 ± 69	471 ± 31

B)				
% RBCs	Fiber number heterogeneity		Protein density heterogeneity	
	Average % change from control (0% RBCs)	P-value	Average % change from control (0% RBCs)	P-value
0%	0% ± 0.1%	-	0% ± 0.3%	-
2%	−3% ± 2%	0.35	5% ± 5%	0.40
10%	22% ± 7%	0.09	46% ± 18%	0.12
20%	18% ± 6%	0.09	21% ± 8%	0.12

Table 2
Fiber diameters measured from scanning electron micrographs

We measured fibrin fiber diameters in four separate experiments (2–5 images acquired per clot and ~100 fibers measured per clot). Because of variability in the control samples (see *Results*), we determined the percent difference from the appropriate control for each fiber measured. The average difference ± standard error of the mean for each %RBCs is shown. P-values were obtained for comparison of these difference values with those from the 0% RBC control sample using an independent Student's t-test.

% RBCs	% Difference from control diameter	P-value
0%	0% ± 1%	-
2%	11% ± 2%	0.006
10%	17% ± 3%	0.008
20%	20% ± 6%	0.048